Postharvest Biology and Technology 230 (2025) 113779

Contents lists available at ScienceDirect

Postharvest Biology and Technology

journal homepage: www.elsevier.com/locate/postharvbio

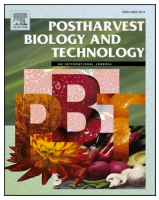

Exploring the biochemical, technical and applicative characteristics of pullulan produced by different strains of *Aureobasidium pullulans*

R. Cignola [a], L. Palou [b], B. Perez-Gago [b], D. Lovison [a], M. Di Foggia [c], F. Basso [a], E. Daniso [a], L. Garagozzo [d], R. De Marco [a], A. Colautti [a], G. Firrao [a], A. Di Francesco [a,*]

[a] Department of Agricultural, Food, Environmental and Animal Sciences, University of Udine, Udine 33100, Italy
[b] Centre de Tecnologia Postcollita (CTP), Institut Valencià d'Investigacions Agràries (IVIA), Montcada, Valencia 46113, Spain
[c] Department of Biomedical and Neuromotor Sciences, University of Bologna, Bologna 40127, Italy
[d] Institute of Science, Technology and Sustainability for Ceramics (ISSMC), National Research Council (CNR), 48018, Italy

ARTICLE INFO

Keywords:
Aureobasidium pullulans – Polysaccharide – Postharvest – Coating – Fruit

ABSTRACT

Pullulan is a polysaccharide with multiple beneficial properties that makes it perfect for several applications and for the food industry. The polysaccharide is produced by *Aureobasidium pullans,* a black yeast also known for its antagonistic properties against plant fungal pathogens. Ten strains, isolated from different environments, were evaluated for their pullulan producing ability. Three strains were selected as main producers (AP1, UOR18, M13). The *pgm1* and *ugp* genes expression was evaluated, showing a significant difference between the strains. Pullulan produced by the strains was biochemically characterized by FT-IR (Fourier Transform Infrared Spectroscopy), DSC (Differential Scanning Calorimetry) and NMR (Nuclear Magnetic Resonance) analyses. By FT-IR and DSC analysis, the AP1 pullulan displayed to be more capable to entrap moisture in its structure, and by NMR, it showed to be more similar to the commercial pullulan. The biopolymer was formulated as apple coating, used to control *Colletotrichum acutatum* by *in vitro* and *in vivo* assays. The coating was activated by yeast cells that enhanced the antifungal activity of the treatment.

1. Introduction

Pullulan is a tasteless, odorless, non-toxic, non-hygroscopic polysaccharide, and safe for human consumption. Due to its edible nature, since 2002, the Generally Recognized as Safe (GRAS) label granted by the US Food and Drug Administration (US FDA) recognized this polymer as an ideal substance for application in various food-related sectors (Raychaudhuri et al., 2020; Mishra et al., 2011). Usually, its white or off-white colour makes it perfect for food industry applications (Prajapati et al., 2013). Pullulan physiochemical characteristics make it also a valuable choice for several applications in the medical and cosmetic sectors (Aquinas et al., 2024; Wani et al., 2021). The molecular structure of pullulan grants high solubility, flexibility, transparency, and a unique film-forming ability (Aquinas et al., 2024), also exploited as drug carriers and capsules (Aquinas et al., 2024). The polymer is composed of α-(1, 6) and α-(1, 4) maltotriose subunits produced by the yeast-like fungus *Aureobasidium pullulans* (de Bary) G. Arnaud (Cheng et al., 2011), also known for its pronounced antagonistic activity against fruit postharvest fungal pathogens (Di Francesco et al., 2023). In recent years, packaging dominates primary plastics use (Geyer et al., 2017), mainly for its physical and mechanical properties and integration into production processes (Marsh and Bugusu, 2007). Nevertheless, these polymers derive from conventional resources, and their processing results in the emission of harmful substances to the environment and human health (Diab et al., 2001a, 2001b). Due to the increased awareness regarding the risks associated with synthetic polymers and pesticides, consumers are shifting their choices to sustainable alternatives (Pooja Saklani et al., 2019; Yadav et al., 2022). As reported by many authors, pullulan could represent a sustainable alternative as coating polymer (Farris et al., 2014; Freitas et al., 2014). In effect, pullulan was particularly suggested to be used as edible coatings of fruits and vegetables, for its technical properties to control moisture and gases exchanges, enhancing products quality and extending shelf life (iab et al., 2001a, 2001b). Also, pullulan has additional advantages over other polysaccharides, such as high transparency, heat sealability and high miscibility with other biopolymers, and not least tasteless and colourless (Biliaderis et al., 1999). As reported by Yuen (1974), pullulan is an excellent vehicle for bioactive compounds. In effect, to promote

* Corresponding author.
E-mail address: alessandra.difrancesco@uniud.it (A. Di Francesco).

https://doi.org/10.1016/j.postharvbio.2025.113779
Received 26 January 2025; Received in revised form 19 June 2025; Accepted 13 July 2025
Available online 15 July 2025

fruit storage by limiting the development of fungal diseases, pullulan is often joined with active substances such as polyphenols (Kang et al., 2023), essential oils (Luís et al., 2020), and chitosan (Kumar et al., 2018). Another valid alternative strategy could be represented by the combination of the polymer with biocontrol agents (BCAs) characterized by effective activity against one or more postharvest fungal pathogens (Settier-Ramírez et al., 2022). As reported by Guimarães et al. (2018), the edible films and coatings could represent a good strategy to apply BCAs on food products because the polymer could be used as a microorganism carrier that improve its viability and efficacy during the storage time. Different authors reported the potential antimicrobial activity of edible films mainly added with lactic acid bacteria to use in food systems (Concha-Meyer et al., 2011; Sánchez-González et al., 2013, 2014).

However, the production of pullulan depends on the microbial strain. It is known that *A. pullulans* strains could display differences in the biosynthetic mechanisms of pullulan production, probably due to different metabolic pathways and cells morphology (Sugumaran and Ponnusami, 2017).

For these reasons, the objectives of the present study were: *i)* to evaluate the pullulan production of 10 different strains of *A. pullulans; ii)* to evaluate the polymer chemical-physical characteristics, *iii)* to develop antifungal pullulan coatings containing yeast cells as BCAs and *iv)* to assess its antifungal activity against a postharvest apple pathogen, *Colletotrichum acutatum,* through *in vitro* and *in vivo* assays.

2. Materials and methods

2.1. Pullulan production by Aureobasidium pullulans strains

Ten strains, molecularly identified as *A. pullulans* (Cignola et al., 2023; Tulukoğlu-Kunt et al., 2023) and belonging to the mycological collection of the Department of Agricultural, Food, Environmental and Animal Sciences (Di4A) of Udine University, were selected for a preliminary screening of pullulan production (Table 1). Pullulan production screening was carried out using the methodology described by Jiang (2010), consisting of 5 days of fermentation and subsequent pullulan precipitation in ethanol. The growing medium was composed of: sucrose 50 g, yeast extract 2 g, KH_2PO_4 5 g, KCl 0.5 g, $MgSO_4 \bullet 7\ H_2O$ 0.2 g, and NaCl 1 g per 1 L of distilled water. The broth was sterilized and aliquots of 50 mL were inserted in sterile flasks. Each flask was inoculated with yeast cells suspensions obtained from 48h-old cultures grown on NYDA plates (8 g Nutrient broth, 5 g Yeast extract, 10 g Dextrose in 1 L of distilled water) (Oxoid, UK) by maintaining the final concentration of 1×10^8 cells/mL. After 5 days in constant agitation (150 rpm) at 20 °C, the fermentation liquid was firstly inactivated at 80 °C for 20 min and then centrifuged at 4000 rpm for 20 min to remove the cells, as reported by Ju et al. (2015). The supernatant was mixed with ethanol (1:2, v:v), as described by Jiang (2010) and then stored overnight at 4 °C. The alcoholic solution with the precipitated pullulan was then centrifuged at 4000 rpm for 20 min to separate the polymer from the liquid. Pullulan was dried in an oven at 80 °C until constant weight, purified by water washing, re-precipitated in ethanol (Hamidi et al., 2019), and later weighed to determine the best pullulan-producing strains. Three flasks were used for each strain.

2.2. Aureobasidium pullulans RNA extraction and gene expression

Yeast strains AP1, UOR18, and M13 were selected as the greater pullulan-producing strains and grown in the same liquid medium described in paragraph 2.1 for 5 and 7 days, respectively. Collected cells were stored at −80 °C, and the RNA was extracted using Spectrum™ plant Total RNA kit (Sigma-Aldrich Co., USA). The concentration and quality of RNA samples were verified using the NanoDrop ND-1000 spectrophotometer (ThermoFisher Scientific, Inc., Wilmington, DE, USA). The cDNA was reverse transcribed using the iScript cDNA Synthesis Kit (Biorad Srl, Milano, Italy). The obtained cDNA was kept at −20 °C until further analysis. The target genes selected and evaluated for pullulan production were α-phosphoglucose mutase (*pgm1)* and UDP-glucose pyrophosphorylase (*ugp*) genes; while actin (*act1)* and elongation factor (*EF1α)* genes were selected as housekeeping genes (HKGs) (Hamidi et al., 2019; Muszkieta et al., 2014) (Table 2). RT-qPCR was performed in a final reaction volume of 20 μL per reaction in a 96-well Bio-Rad CFX96 Real-Time PCR System (Bio-Rad Inc., Hercules, CA, USA) in white-walled PCR plates with clear adhesive sealers. Reaction mixtures contained 0.2 μM each primer, SYBR SsoFast™ EvaGreen (Biorad Srl, Milano, Italy), molecular grade H_2O, and 5 ng of cDNA. The cycling conditions were 30 s at 95 °C, followed by 40 cycles of 5 s at 95 °C and 5 s at 60 °C. For each strain, three biological and technical replicates were considered.

2.3. Chemical analyses

2.3.1. FT-IR pullulan analysis

Pullulan produced by AP1, UOR18, M13 (1 g) strains and a commercial one (TCI, Japan) (standard, STD) were collected in sterile tubes (2 mL) and stored at −80 °C and quickly lyophilized. Pullulan samples were analyzed by FT-IR spectroscopy to obtain a rapid biochemical characterization of their main molecular components and to study their differences. After homogenization by vortexing, infrared spectra were recorded with an FT-IR spectrophotometer (IR-TRACER-100, Shimadzu, Tokyo, Japan) equipped with an attenuated total reflectance (ATR-Diamond crystal) apparatus. The spectra were collected from 4000 to 400 cm^{-1} and averaged over 100 scans (resolution = 4 cm^{-1}); three spectra were measured for each sample.

2.3.2. Pullulan NMR spectroscopy

Nuclear magnetic resonance (NMR) spectra of AP1, UOR18, M13, and STD pullulans were recorded on a Bruker AV 400 at ambient temperature (400.13 MHz for ^1H NMR and 100.53 MHz for $^{13}C\{^1H\}$ NMR. Chemical shifts δ are reported in ppm with respect to residual ^1H and ^{13}C signals of the deuterated solvents as an internal standard, whereas coupling constants J are denoted in hertz (Hz). $^{13}C\{^1H\}$ NMR spectra were baseline-corrected, and occasionally exponential apodization functions were used to improve resolution.

Table 1
Aureobasidium pullulans strains evaluated for pullulan production.

Strain	Source	Reference
AL25	Laurel leaf	Cignola et al., 2023
AP1	Apple fruit	Cignola et al., 2024
M13	Apple fruit	Tulukoğlu-Kunt et al., 2023
SE0	Plum pulp	Cignola et al., 2023
UC11	Olive leaf	Cignola et al., 2023
UC14	Olive leaf	Cignola et al., 2023
UC22	Olive leaf	Cignola et al., 2023
UOR112	Olive leaf	Cignola et al., 2023
UOR18	Olive leaf	Cignola et al., 2023
VB23	Viburnum leaf	Cignola et al., 2023

Table 2
RT-qPCR primers.

Gene	Primer	Sequences, 5′ → 3’	Reference
Act1	Fw	GTTGTCCCCATCTACGAAGGTTTC	Hamidi et al.,
(HKG)	(ACTIN1)		2019
	Re	GCTTCTCCTTGATGTCACGAACG	
	(ACTIN1)		
EF1α	Fw (EF1α)	CCATGTGTGTCGAGTCCTTC	Muszkieta et al.,
(HKG)	Re (EF1α)	GAACGTACAGCAACAGTCTGG	2014
Pgm1	Fw(PGM1)	GAGTCCTTCGTTACCAGCATTC	Ju et al., 2015
	Re(PGM1)	GAGTGACCTCAGGGTTCCAGTA	
Ugp	Fw(UGP)	TCATCCCCAACGGCAAGTCG	Hamidi et al.,
	Re(UGP)	AGCATCAAGTCGGAGCAGGTC	2019

2.3.3. Thermal analyses on pullulan samples

Thermal analyses were conducted using a DSC-3 StarE system (Mettler-Toledo, Greifensee, Switzerland). The instrument temperature calibration was carried out using hexane (melting point: −93.5 °C), double-distilled water (melting point: 0.0 °C), and indium (melting point: 156.6 °C). Heat flow calibration was achieved using indium (heat of fusion 28.45 J/g). Approximately 10 mg of each pullulan sample (AP1, UOR18, M13, and STD) were weighed inside 100 μL aluminum pans (Mettler-Toledo). Samples were allowed to equilibrate at 10 °C for 2 min and then heated from 10 to 300 °C at 10 °C/min. The entire analysis was conducted under constant nitrogen flow (20 mL/min) to prevent any oxygen-dependent undesired reaction. An analogous empty pan was used as a reference for the analysis. Glass transition temperature (T_g, °C), peak onset (T_{on}, °C), peak temperature (T_{peak}, °C), and melting enthalpy (ΔH, J/g) were computed from the thermograms using the StarE software (v.8.10, Mettler-Toledo).

2.4. Pullulan active film vitality

The film-forming solution (FFS) was prepared with 3 % of each pullulan from the strains AP1, UOR18, M13, glycerol (Fisher Bioreagents, USA) 0.6 % as a plasticizer, and 0.05 % of Tween 20 (Sigma-Aldrich, USA) (wb, wet basis). The viscosity of the solution was measured using a rotational viscosimeter with an LCP probe. Antifungal coatings were formulated by adding AP1, UOR 18 and M13 cells as BCAs, collected after 48 h of growth in NYDB (NYDA without agar). The final concentration of the active FFS was 1×10^8 cells/mL. The FFSs were finally dried under a laminar flow hood inside sterile Petri dishes (90 mm, Ø), and incubated at 20 °C with 43 % of R.H. (relative humidity). The cell vitality of the strains was evaluated weekly for one month. Each film was dissolved in 1 mL of sterile water, and 5-fold dilutions were subsequently made. Then, 100 μL of each dilution were plated on NYDA plates and incubated at 25 °C for 2 days. The sample unit for each dilution and film consisted of 3 plates.

2.4.1. In vitro antifungal activity of pullulan films

The antifungal activity of the non-activated (without BCA cells) and active films was evaluated, as reported by Settier-Ramírez et al. (2022). Firstly, 18 g of FFS were dried in a Petri dish (90 mm) to obtain the final films. Subsequently, sterilized food-grade cellophane (Pacifici, Italy) of the same plate diameter was placed on the PDA medium (Potato Dextrose Agar, 39 g/L) (Oxoid, UK) surface. Cellophane was used to prevent the film from contact with the agar medium (De Araújo and Roussos, 2002). Cellophane was covered with dried films, and mycelial plugs (6 mm diameter) from a 7 days old colony of *Colletotrichum acutatum* D3-A (isolated from apple cv 'Golden Delicious', and belonging to mycological collection of DI4A, University of Udine), previously grown on PDA at 25 °C, were placed in the center of the Petri dishes. Plates were closed with parafilm to avoid dehydration and incubated at 20 °C. The experiment was conducted twice. The sample unit was represented by 3 plates. Plates containing PDA and sterile cellophane disks were used as controls.

2.4.2. In vivo antifungal activity

The antifungal activity of the FFS was evaluated on apples cv 'Pink Lady'. Fruits were harvested in an orchard located in Codroipo, Friuli Venezia Giulia Region (Italy), at commercial maturity (10–11 °Brix). Prior to coating, apples, homogeneous in size and without lesions or rots, were surface disinfected by immersion in a 1 % sodium hypochlorite solution for 1 min, rinsed with tap water, and finally dried at room temperature. One wound per fruit was artificially made with a sterile plastic needle (2 mm Ø). Each wound was inoculated with 20 μL of *C. acutatum* D3-A conidial suspension (1×10^4 conidia/mL) 4 h before (curative application) or 24 h after (preventative application) the treatment. Conidia were collected from strain D3-A colony, previously grown on PDA at 25 °C for 1 week, and suspended in sterile water containing 0.05 % (v/v) Tween80. The suspension was adjusted to the final concentration (1×10^4 conidia/mL) using a haemocytometer.

The treatment consisted of 400 μL of FFS pipetted onto each fruit and rubbed with gloved hands to simulate the application by rolling brushes of coating machines used by the fresh fruit industry (Karaca et al., 2014). Apples were incubated at 20 °C and 80 % R.H. and fungal disease incidence (%) and severity (mm) were evaluated after 1 week. The FFSs created using pullulan from the different yeast strains (AP1, UOR18, and M13) with and without the relative cells were used as treatments. Apples inoculated only with the pathogen were used as untreated controls. The experiment was conducted twice. The sample unit consisted of 3 replicates of 20 apples.

2.5. Statistical analyses

All the data were analyzed using ANOVA one-way analysis. The separation of means was performed with Tukey's test ($\alpha = 0.05$ and $\alpha = 0.01$) by using the software MiniTab.17. Data were reported as mean values ± standard error (SE). Gene expression data analyses were performed using CFX Maestro™ Software (Biorad Srl, Milano, Italy)

3. Results

3.1. Pullulan production

Pullulan production was assessed to determine which strains, belonging to our collection, were the most active, in terms of polysaccharide production yield. The highest quantity was displayed by the AP1 strain, with 11.43 g of pullulan from 1 L of fermentation medium (Table 3). Strains UOR18 and M13 were the second and third most pullulan productive, respectively, with 6.7 g/L and 3.07 g/L.

3.2. Gene expression analysis

Pgm1 and *ugp* are two of the most important genes involved in the metabolic pathway of *A. pullulans* for pullulan production (Hamidi et al., 2019). In Fig. 1, the expression levels of both genes by the most productive pullulan strains are reported. Regarding the *pgm1* gene, all the strains showed a significantly higher expression after 7 days of fermentation compared to 5 days. The expression value of the gene, after 7 days of fermentation, was 2, 3, and 4 times higher with respect to that of 5 days, respectively for AP1, M13, and UOR18. However, the AP1 strain displayed after 5 days of fermentation the highest *pgm1* expression level. Conversely, for the *ugp* gene, the expression level was higher after 5 days of fermentation if compared with 7 days, except for the AP1 strain, which was confirmed to be the strain with the highest levels of *ugp* gene expression. Of the three *A. pullulans* strains, M13 had the lowest gene expression levels.

Table 3
Pullulan production (g/L) by *Aureobasidium pullulans* strains after 5 days of fermentation. Different letters indicate significant differences according to Tukey's test ($\alpha = 0.05$).

A. pullulans strain	Pullulan yield (g/L)
AL25	2.73 ± 0.03 cd
AP1	11.43 ± 0.07 a
M13	3.07 ± 1.22 c
SE0	2.15 ± 0.02 def
UC11	1.95 ± 0.04 ef
UC14	1.13 ± 0.02 g
UC22	1.5 ± 0.05 fg
UOR112	2.12 ± 0.15 def
UOR18	6.17 ± 0.34 b
VB23	2.62 ± 0.16 cde

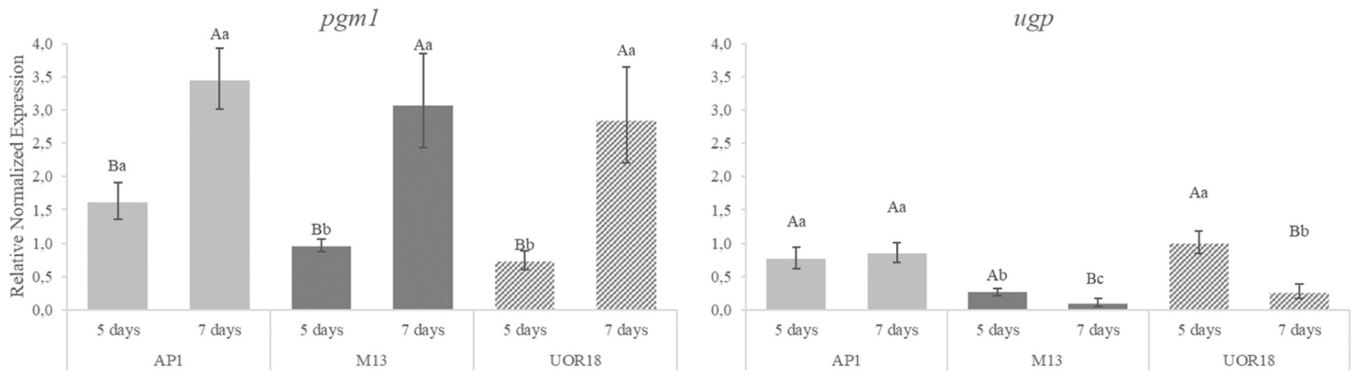

Fig. 1. Gene expression levels of the *pgm1* and *ugp* genes normalized with respect to the housekeeping gene *act1 and EF1α*. Data shows the relative gene expression of *Aureobasidium pullulans* strains after 5 and 7 days of fermentation. Different uppercase letters indicate significant differences within the same strain at different times and lowercase letters between different strains at the same time, according to Tukey's test ($\alpha = 0.05$).

3.3. Chemical characteristics

3.3.1. FT-IR

The IR spectra of the solid standard pullulan, together with that produced by the AP1, M13, and UOR18 strains, are presented in Fig. 2. The attribution of IR pullulan bands was based on previous literature (Saber-Samandari et al., 2014; Shingel, 2002; Synytsya and Novak, 2014). The IR spectra allowed us to detect the α-(1→4) and α-(1→6) glycosidic bonds present in pullulan. The first type of bond showed the characteristic bands at 995, 849, and 756 cm^{-1}. At the same time, the second appeared at 1076 and 930 cm^{-1} and was observed in all pullulan samples regardless of their origin, indicating an overall good purity of the extracted pullulan. These latter showed a general slight intensity decrease compared to the standard sample that was more evident for

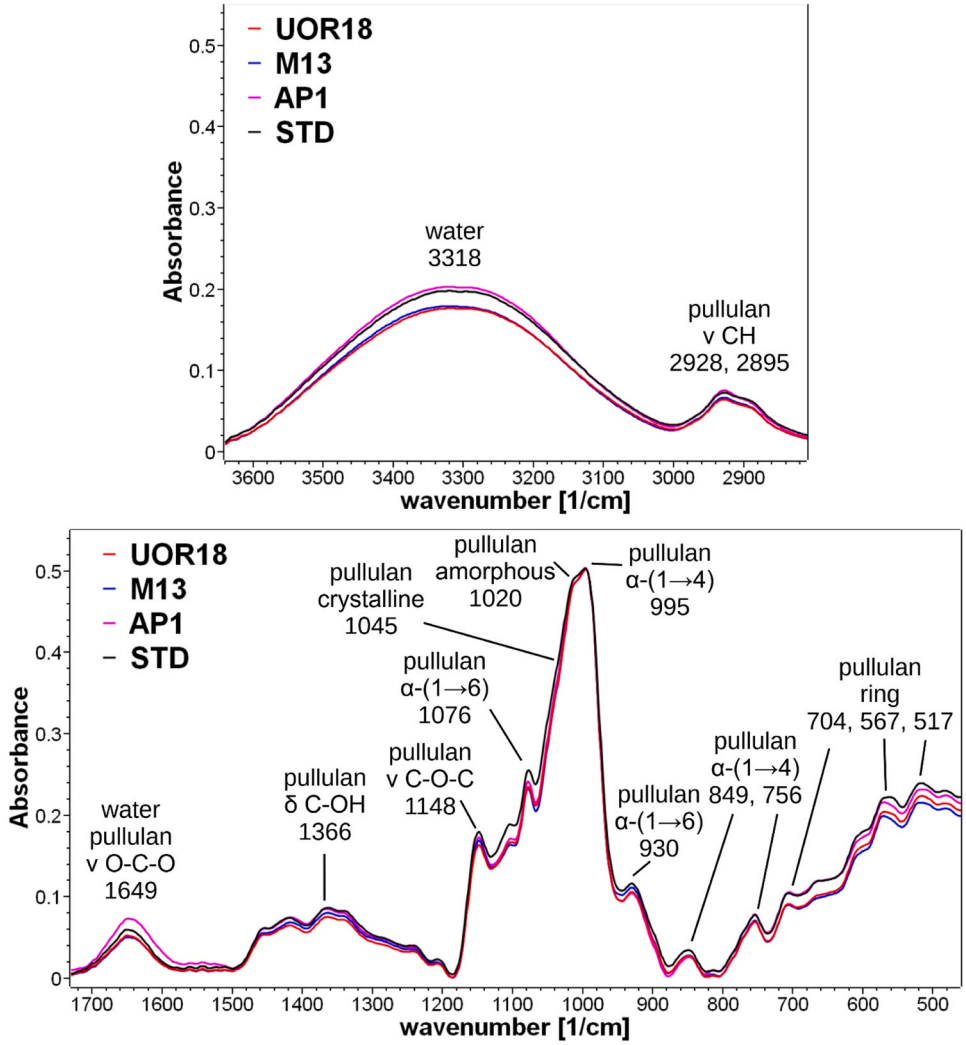

Fig. 2. IR spectra of the solid standard pullulan (STD), together with that produced by the AP1, M13, and UOR18 *Aureobasidium pullulans* strains.

bands attributed to α-(1→6) glycosidic bond (1076 and 930 cm^{-1}), which may indicate a specific cleavage of this kind of bond (Shingel, 2002). Consequently, the band at 1148 cm^{-1} decrement, is attributed to the formation of glycosidic bonds between maltose units (Shingel, 2002). In analogy with starch, the IR bands at 1045 and 1020 cm^{-1} were attributed to crystalline and amorphous domains of pullulan, respectively (Shingel, 2002). The intensity of the first band is not easy to evaluate since it is a shoulder of the main band with a peak at 995 cm^{-1}. Therefore, it is difficult to determine whether a change in crystallin order occurred in the extracted samples. Given the similarities as mentioned earlier, AP1 pullulan was the most similar to the standard pullulan and the one containing the most water (i.e., the 3318 and 1649 cm^{-1} water bands are the most intense).

3.3.2. Thermal analyses of pullulan

The differential scanning calorimetry analysis of pullulan samples resulted in thermograms showing the typical pullulan thermal behavior (Karim and Islam, 2011; Poudel et al., 2020; Singh and Kaur, 2019). In particular, a large, broad endothermic peak in the first part of the considered temperature range (i.e., 25–150 °C) was clearly visible (Fig. 3). According to the literature, this peak was due to the evaporation of water still present as embedded within the pullulan matrix (Shah et al., 2020; Singh et al., 2019). Despite not providing direct information on the polymer structure, differences in the shape of this peak can indicate a different ability of the materials to entrap water. In particular, it is clearly visible that the STD, M13, and UOR18 pullulan samples showed a peak ending at ~ 140–160 °C, whereas pullulan produced by AP1 strain exhibited a water evaporation band stretching up to 200 °C. Based on these data, it can be inferred that the AP1 sample was much more capable of entrapping moisture in its structure than the other three matrices.

3.3.3. Pullulan NMR analysis

The investigation of the profile of ^{1}H-signals in NMR experiments offers a general fingerprint of the studied molecule in solution, providing useful information concerning the degree of purity, structural features, and dynamic properties of specific regions or sites within a molecule. Therefore, the extracted pullulan from AP1, M13, and UOR18 strains were investigated by ^{1}H, ^{13}C, and ^{2}D NMR spectroscopy in D_2O for structural characterization and thus compared to standard pullulan (STD). Generally, pullulan is a polysaccharide having repeating maltotriose units connected via both α-(1→6) and α-(1→4) linkages (Fig. 4A), indeed according to the ^{1}H NMR spectra, all the samples revealed the presence of α-(1→6) and α-(1→4) linkages in the ratio of 1:2, exhibiting the α-(1→6) linkages between every third glucose ring. On the basis of chemical shifts, the signals at δ = 5.32 and 5.28 ppm were attributed to the anomeric protons in 1B and 1 C positions (Fig. 4B), supporting the formation of α-(1→4) linkages. Conversely, the peak at δ = 4.87 ppm is due to anomeric proton 1 A at the site of the α-(1→6) linkage, while site 4 is also clearly evident at δ = 3.39 ppm (Fig. 4B).

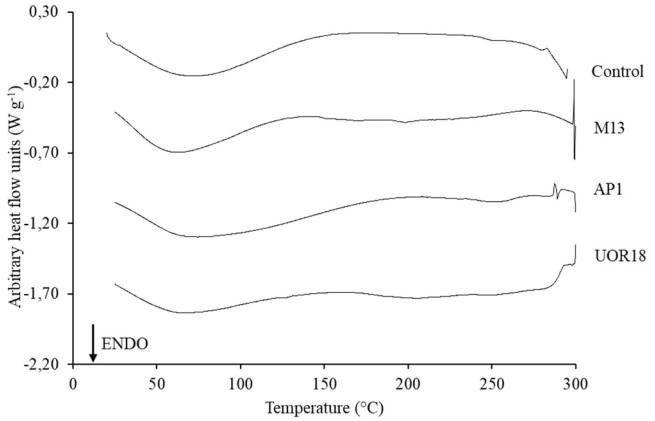

Fig. 3. Thermograms of pullulan samples.

Although ^{1}H NMR spectra are quite informative in terms of the general view of the molecule, fully protonated molecules with high-molecular weights, result in very complex ^{1}H NMR spectra. This can be noticed by the presence of many overlapped and, thus, unresolved peaks with no clear structural pattern. In general, in polysaccharide analysis, except for the ^{1}H-signals belonging to the anomeric, all other ring protons from the monosaccharides resonate very close, as demonstrated by the ^{1}H NMR region ranging from δ = 4.00–3.45 ppm where protons of sites 2, 3, 5 and 6 are found (Fig. 4B). Therefore, the investigation of other nuclei, such as ^{13}C, either coupled or uncoupled to ^{1}H, becomes valuable and complementary in the analyses, providing important remarks. With that said, ^{13}C and 13C-1H correlation experiments were also performed. The anomeric carbon atoms of the studied polysaccharides have been observed in ^{13}C NMR experiments (Figures S1-S4), where the anomeric α-(1→6) carbon signals were found at δ = 97.91 ppm for 1 A, while the anomeric α-(1→4) carbons at δ = 99.75 and 100.21 ppm for sites 1 C and 1B, respectively. Finally, the correlation between the anomeric protons and carbons was confirmed by 13C-1H HSQC NMR measurements (Figures S5-S8). More importantly, minor peaks were observed in the case of samples M13 and UOR18 at δ = 5.14 and 4.55 ppm in ^{1}H NMR experiments, and at δ = 95.88 and 92.02 ppm in ^{13}C NMR spectra, most likely due to the anomeric proton and carbon of the terminal glucose rings in α and β configurations, respectively (Figs. 4C and 4D). In addition to chemical shifts, they exhibit very different 1–1 H J-coupling constants due to the rotational angle between the coupled protons. Indeed, the β-anomer has a much larger coupling constant (7.7 Hz) than the α-anomer (3.9 Hz). The ratio between the anomeric protons of the maltotriose units (protons 1 A, 1B, and 1 C in Fig. 4A) and the anomeric proton of the terminal glucose is strictly related to the degree of polymerization (DP) of the pullulan. According to the integrals of the above-mentioned anomeric peaks, it is possible to measure the yield of the polymer formation, being 90 % for M13 and 97 % for UOR18, and calculate the DP using Carothers' equation:

$$\overline{X}_n = \frac{1}{1-p}$$

where $\overline{X}_n$ gives the number of maltotriose units in the average chain, whereas p is a measure of the extent of the reaction or yield. The calculated DP was found to be 6.67 for M13 and 33.33 for UOR18, while no minor peaks belonging to terminal glucose units were observed in the case of AP1, the latter resulting in the most similar polysaccharide to the standard STD pullulan.

3.4. Vitality and antifungal efficacy of active pullulan films

The vitality of the activated pullulan films formulated with AP1, UOR18, and M13 cells as BCAs was successfully evaluated for over one month of storage at 20 °C and 43 % of R.H., remaining significantly stable (data not shown). For this reason, the active films were used to evaluate the inhibition of *C. acutatum* mycelial growth on PDA medium. *In vitro* assays results highlighted a positive inhibitory effect of the active films against the fungal growth. Interestingly, no inhibition was detected with non-active pullulan film. Conversely, all the active films (with BCAs cells) inhibited the pathogen growth by 55 % and 53 %, respectively for AP1, M13, and UOR18, with no statistical differences from each other among them (Fig. 5).

3.5. Antifungal activity of pullulan coatings: in vivo assay

The non-active and active coatings, applied on apples as a preventative treatment, were able to reduce both the lesion diameter and the disease incidence (Fig. 6). The AP1 active coating reduced the incidence

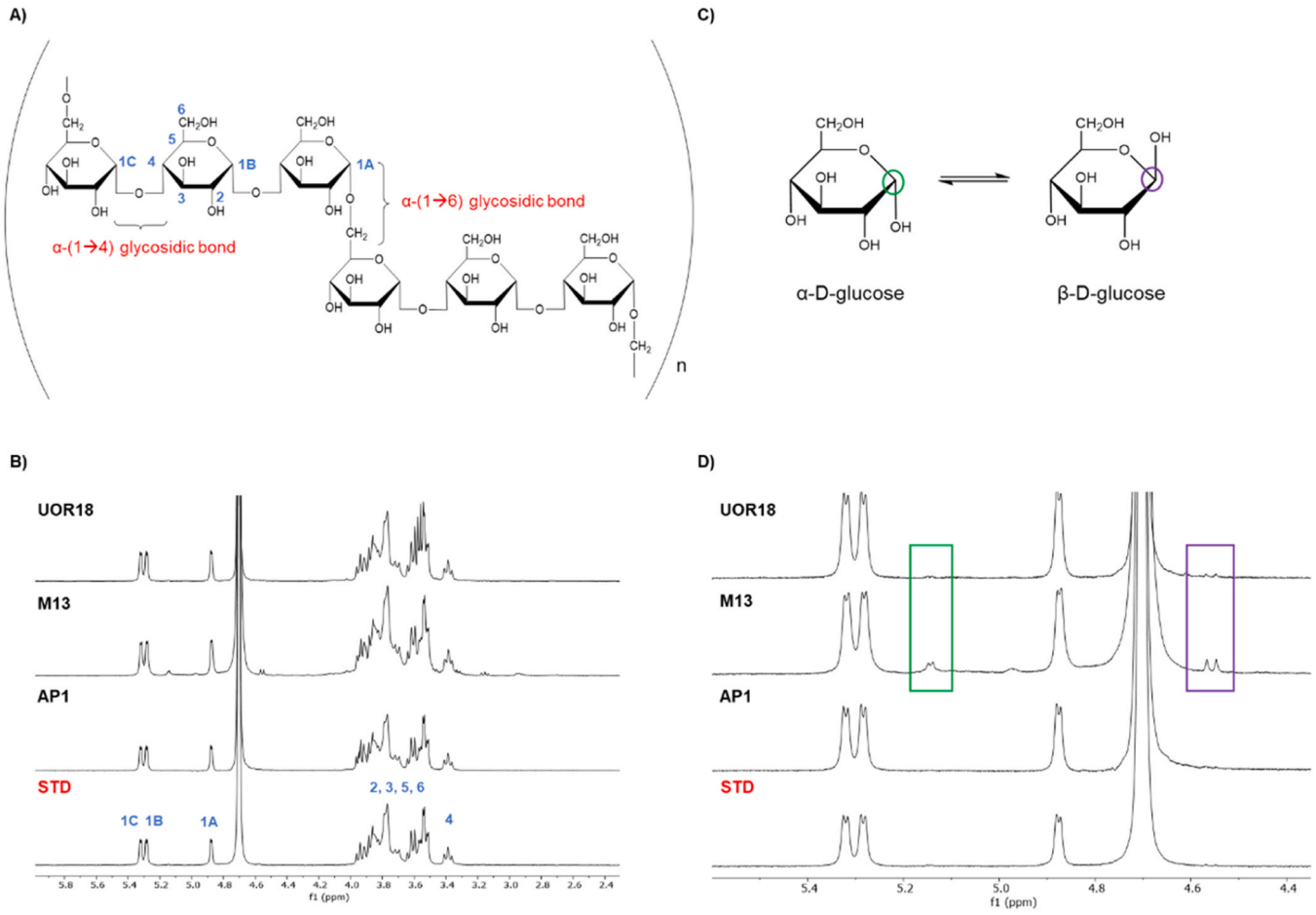

Fig. 4. A) Chemical structure of pullulan where α-(1→4) and α-(1→6) linkages are highlighted, in addition to the main sites of the maltotriose unit marked as 1 A, 1B, 1 C, 2, 3, 4, 5, and 6. B) Stacking ^{1}H NMR spectra of the studied pullulans STD, AP1, M13, and UOR18. C) Chemical structures of glucose α and β conformations; anomeric sites have been circled in green and purple for the α and β anomers, respectively. D) Stacked ^{1}H NMR spectra of pullulans in the region $\delta = 5.6 - 4.4$ ppm. The presence of the glucose anomeric protons in both α and β configurations have been marked with green (α configuration) and purple (β configuration) boxes.

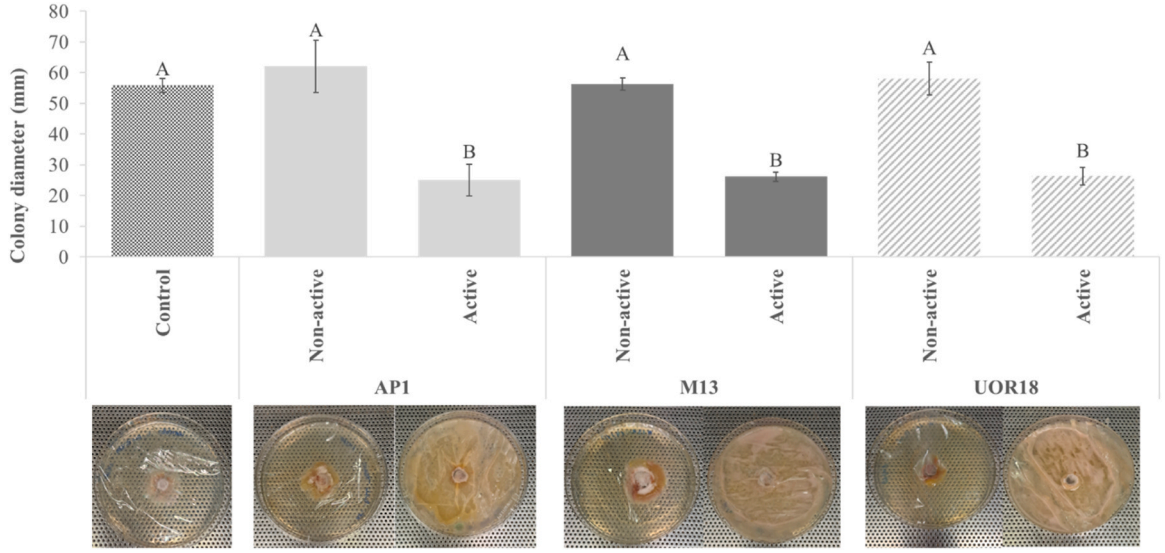

Fig. 5. *Colletotrichum acutatum* colony growth (mm) on non-active and active pullulan films. Different letters indicate significant differences according to Tukey's test ($\alpha = 0.05$).

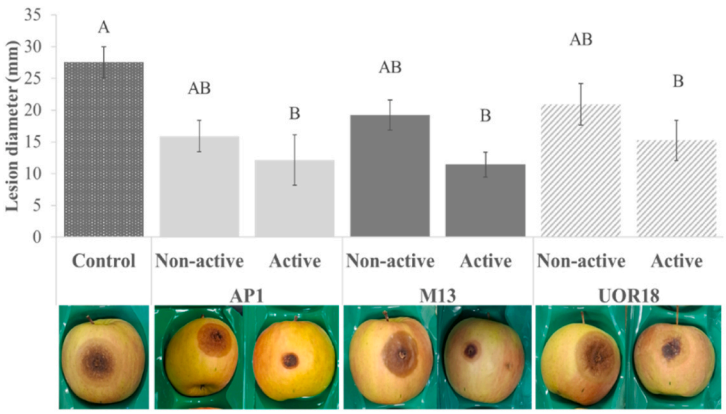

Coating	Disease Incidence (%)
Control	100
AP1 Non-active	67
AP1 Active	44
M13 Non-active	78
M13 Active	89
UOR18 Non-active	89
UOR18 Active	67

Fig. 6. Efficacy of non-active and active pullulan coatings against *Colletotrichum acutatum* D3-A on apples (disease severity, mm, and incidence, %) as preventative treatment. Different letters indicate significant differences according to Tukey's test ($\alpha = 0.05$).

of bitter rot disease by 56 %. The lesion diameter was reduced by 55 % by the same treatment. The M13 and UOR18 active films inhibited the pathogen incidence by 11 % and 33 %, respectively. No significant differences were detected among the different treatments with the active films coatings for the lesion diameter. Coatings, non-active and active, obtained from M13 and UOR18 strains applied as curative treatment were not effective in containing *C. acutatum*. Instead, AP1 active coating was able to reduce disease incidence by 11 % (data not reported).

4. Discussion

Synthetic polymers are gradually being replaced by biodegradable compounds, mainly derived from renewable natural resources (Kumar et al., 2023). Pullulan is a biopolymer known for its chemical-physical characteristics and non-toxic properties, which make it a viable alternative for sustainable food packaging and coating (Dewan and Islam, 2024).

The present study analyzed the different capabilities of ten *A. pullulans* strains to produce this biopolymer. The yeast strains were isolated from different plant sources located Italy and Turkey (Cignola et al., 2023; Tulukoğlu-Kunt et al., 2023), and all demonstrated a capacity to produce pullulan, despite lower production than other strains used in other studies (Hamidi et al., 2019; Prasongsuk et al., 2007) was detected. However, the three strains AP1, UOR18, M13 and their relative polysaccharides were chosen for the highest production yield, and particularly the *A. pullulans* AP1 strain.

The analysis of *pgm1* and *ugp* genes, known to be a key factor in the synthetic pathway of pullulan (Wang et al., 2015), partially confirmed the yield results obtained. In fact, the gene expression levels displayed that a longer fermentation could increase the overexpression of the *pgm* gene, particularly in the strain AP1. Conversely, UDPG-pyrophosphorylase (*ugp*) gene expression decreased, however, only for M13 and UOR18 strains. As reported by (Guo et al. (2018), pullulan production can significantly increase, almost by 17 %, with the overexpression of UDPG-pyrophosphorylase. Also, Guo et al. (2018) affirmed that the overexpression or deletion of other genes exerted little effect on pullulan biosynthesis. In fact, from our results, the pullulan yield by AP1 and UOR18 strains was notably higher than the M13 strain. After determining the best *A. pullulans* producers of the target polymer, our study aimed to verify the biochemical and technological potentialities of the obtained molecule. FTIR NMR, and DSC analysis were used to complement the characterization of the chemical composition and thermal properties of the obtained pullulans. All three analytical techniques underscore that all the extracted pullulans were quite similar among them and to the standard. However, some chemical differences could explain the different behavior of the extracted pullulans in *in vitro* and *in vivo* assays. More in detail, FTIR and DSC pointed out that the AP1 pullulan contained the most water (Figs. 2 and 3), while FTIR and NMR showed that the AP1 was the most similar to the standard pullulan (Figs. 2 and 4). The DSC thermogram revealed the presence of an endothermic peak, whereby pullulan produced by AP1 strain seemed to exhibit a water evaporation band stretching up to 200 °C. Through this, pullulan produced by the AP1 strain should be more capable of entrapping moisture in its structure. Regarding this, pullulan film with an increase in moisture content could determine large changes in internal fruit atmosphere composition, which were beneficial for extending the shelf-life of fruit. In fact, coated fruit with higher levels of CO_2 and an internal reduction of O_2 display better firmness, color retention, and reduced weight loss (Diab et al., 2001). NMR gave information on the degree of polymerization of pullulan that was lower in M13 and UOR18 compared to AP1 and the standard sample. On the contrary, the FTIR technique can not give direct information on pullulan's polymerization degree. Still, IR spectra showed a decrease in the 1148 cm^{-1} band, attributed to the formation of glycosidic bonds between maltose units (Shingel, 2002) in the M13 and UOR18 samples. The contemporaneous decrease of the typical bands of α-(1→6) at 1076 and 930 cm^{-1} in the same samples indicated a preferential cleavage of this kind of glycosidic bond that led to a decrease in the polymerization degree as observed in NMR spectra of M13 and UOR18 samples.

Our results showed that by incorporating the cells of each pullulan producer strain into the film/coating formulation, the polymers gained efficacy as a potential treatment to prolong fruit shelf life and reduce pathogen incidence, as reported by Settier-Ramirez et al. (2022).

The association of coating matrix together with a BCA cells may provide many advantages, in particular with AP1 strain. It could act as a protective barrier around the microorganism cells (Iñiguez-Moreno et al., 2021), improve the BCA adherence and persistence on fruit surface, increasing the microorganism space colonization so limiting the pathogen infection (Miranda et al., 2024). As reported by Iñiguez-Moreno et al. (2021), an efficient coating polymer can extend the shelf life of BCAs, preserving their viability and effectiveness. In fact, the coating uniformly spread the microorganism cells on fruit surface thus favoring colonization. A previous study, by scanning electron microscopy confirmed the ability of *A. pullulans* to colonize fruit wound and consequently prevent pathogen growth (Di Francesco et al., 2017).

Encouraging results were achieved by incorporating *A. pullulans* AP1 cells in the FFS and into the coating used as a preventative application on apples. Probably the coatings helped the yeast cells to maintain a suitable concentration and stability on apple surface, guaranteeing the active effect of the BCA secondary metabolites against the pathogen. However, integrating the coating directly with antimicrobial compounds produced by *A. pullulans* (Di Francesco et al., 2015, 2020) may enhance its effectiveness against fruit pathogens, as reported by De Oliveira Caretta et al. (2024) on strawberries, where sophorolipids from

Starmerella bombicola and fructooligosaccharides from *B. subtilis* were incorporated into a cassava starch biopolymer coating.

Unfortunately, in our study, no inhibitory effects of *C. acutatum* were obtained by the tested coating as a curative treatment or without BCA cells activation. Conversely, pullulan coating application on table grape displayed a significant efficacy against *Botrytis cinerea* (unpublished results). However, integrating a coating matrix with an active BCA can provide physical improvement and increase the microorganism's survival rate (Lieu et al., 2024). Also, pullulan coating/film guarantees a uniform spread, providing a successful fruit colonization by the BCA (Marín et al., 2016). The application of an active coating inhibits the microbial growth but at the same time create a protective barrier that slow fruit respiration and transpiration (Miranda et al., 2024).

Nevertheless, there are many factors to consider for developing an active coating/film such as the viability and stability of the strain and the total absence of potential food safety hazards. Developing a biopolymer like pullulan with an optimal chemical composition and optimizing costs could represent a significant step forward in food and fruit postharvest management. Improving the fermentation substrate formula could represent a new frontier to look at, as well as the antagonist formulation.

CRediT authorship contribution statement

R.C., and A.D.F: Conceptualization, formal analysis and investigation, writing original draft and methodology. A.D.F.: supervision, writing review and editing, funding acquisition. L.P., B.P.-G. M.D.F. and R.D.M.: review and editing. G.F., D.L., F.B., E.D., L.G. and A.C.: Formal analysis, review and editing.

Funding

Young Researcher Call (YRC) - "iNEST – Interconnected Nord-Est Innovation Ecosystem" – ECS_00000043 - CUP G23C22001130006 - NextGenerationEU.

Declaration of Competing Interest

The authors declare that they have no conflicts of interests.

Appendix A. Supporting information

Supplementary data associated with this article can be found in the online version at doi:10.1016/j.postharvbio.2025.113779.

Data availability

Data will be made available on request.

References

Aquinas, N., Chithra, C.H., Bhat, M.R., 2024. Progress in bioproduction, characterization and applications of pullulan: a review. Polym. Bull. 81, 12347–12382. https://doi.org/10.1007/s00289-024-05300-2.

Biliaderis, C.G., Lazaridou, A., Arvanitoyannis, I., 1999. Glass transition and physical properties of polyol-plasticised pullulan–starch blends at low moisture. Carb. Pol. 40 (1), 29–47.

Cheng, K.-C., Demirci, A., Catchmark, J.M., 2011. Pullulan: biosynthesis, production, and applications. Appl. Microbiol. Biotechnol. 92, 29–44. https://doi.org/10.1007/s00253-011-3477-y.

Cignola, R., Boato, A., Sadallah, A., Firrao, G., Di Francesco, A., 2023. Molecular characterization of *Aureobasidium* spp. strains isolated during the cold season. A preliminary efficacy evaluation as novel potential biocontrol agents against postharvest pathogens. Eur. J. Plant Pathol. https://doi.org/10.1007/s10658-023-02696-x.

Cignola, R., Firrao, G., Freschi, G., Di Francesco, A., 2024. *Aureobasidium pullulans* formulations: evaluation of the effectiveness against grey mould of table grape. J. Plant Pathol. https://doi.org/10.1007/s42161-024-01671-7.

Concha-Meyer, A., Schöbitz, R., Brito, C., Fuentes, R., 2011. Lactic acid bacteria in an alginate film inhibit Listeria monocytogenes growth on smoked salmon. Food Control 22, 485–489.

De Araújo, A.A., Roussos, S., 2002. A technique for mycelial development of ectomycorrhizal fungi on agar media. Appl. Biochem. Biotechnol. 98-100:311-8. doi: 10.1385/abab:98-100:1-9:311.

De Oliveira Caretta, T., Baldo, C., Silveira, V.A.I., Hipólito, A., Costa, N.J.A., Mali, S., Celligoi, M.A.P.C., 2024. Synthesis of novel antimicrobial bioactive films for strawberry coating based on sophorolipids and fructooligosaccharides-modified starch. Polym. Bull. 81, 3563–3581.

Dewan, Md.F., Islam, Md.N., 2024. Pullulan-based films: unveiling its multifaceted versatility for sustainability. Adv. Polym. Technol., 2633384 https://doi.org/10.1155/2024/2633384.

Diab, T., Biliaderis, C.G., Gerasopoulos, D., Sfakiotakis, E., 2001a. Physicochemical properties and application of pullulan edible films and coatings in fruit preservation. J. Sci. Food Agr. 81, 988–1000.

Di Francesco, A., Roberti, R., Martini, C., Baraldi, E., Mari, M., 2015. Activities of *Aureobasidium pullulans* cell filtrates against *Monilinia laxa* of peaches. Microbiol. Res. 181, 61–67.

Di Francesco, A., Ugolini, L., D'Aquino, S., Pagnotta, E., Mari, M., 2017. Biocontrol of *Monilinia laxa* by *Aureobasidium pullulans* strains: Insights on competition for nutrients and space. Int. J. Food Microbiol. 248, 32–38.

Di Francesco, A., Baraldi, E., Di Foggia, M., Zajc, J., Gunde-Cimerman, N., 2020. Study of the efficacy of *Aureobasidium* strains belonging to three different species: *A. pullulans, A. subglaciale* and *A. melanogenum* against *Botrytis cinerea* of tomato. Ann. Appl. Biol. 177, 266–275.

Di Francesco, A., Zajc, J., Stenberg, J.A., 2023. Aureobasidium spp.: diversity, Versatility, and Agricultural Utility. Horticulturae 9, 59. https://doi.org/10.3390/horticulturae9010059.

Diab, T., Biliaderis, C.G., Gerasopoulos, D., Sfakiotakis, E., 2001b. Physicochemical properties and application of pullulan edible films and coatings in fruit preservation. J. Sci. Food Agr. 81, 988–1000. https://doi.org/10.1002/jsfa.883.

Farris, S., Unalan, I.U., Introzzi, L., Fuentes-Alventosa, J.M., Cozzolino, C.A., 2014. Pullulan-based films and coatings for food packaging: Present applications, emerging opportunities, and future challenges. J. Appl. Polym. Sci. 131, 40539. https://doi.org/10.1002/app.40539.

Freitas, F., Alves, V.D., Reis, M.A., Crespo, J.G., Coelhoso, I.M., 2014. Microbial polysaccharide-based membranes: current and future applications. J. Appl. Polym. Sci. 131. https://doi.org/10.1002/app.40047.

Geyer, R., Jambeck, J.R., Law, K.L., 2017. Production, use, and fate of all plastics ever made. Sci. Adv. 3 (7), 25–29. https://doi.org/10.1126/sciadv.1700782.

Guo, J., Huang, S., Chen, Y., Guo, X., Xiao, D., 2018. Discovering the role of the apolipoprotein gene and the genes in the putative pullulan biosynthesis pathway on the synthesis of pullulan, heavy oil and melanin in *Aureobasidium pullulans*. World J. Microbiol. Biotechnol. 34, 11. https://doi.org/10.1007/s11274-017-2398-z.

Hamidi, M., Kennedy, J.F., Khodaiyan, F., Mousavi, Z., Hosseini, S.S., 2019. Production optimization, characterization and gene expression of pullulan from a new strain of Aureobasidium pullulans. Int. J. Biol. Macromol. 138, 725–735. https://doi.org/10.1016/j.ijbiomac.2019.07.123.

Iñiguez-Moreno, M., Ragazzo-Sánchez, J.A., Barros-Castillo, J.C., Solís-Pacheco, J.R., Calderón-Santoyo, M., 2021. Characterization of sodium alginate coatings with *Meyerozyma caribbica* and impact on quality properties of avocado fruit. LWT 152, 112346.

Jiang, L., 2010. Optimization of fermentation conditions for pullulan production by *Aureobasidium pullulan* using response surface methodology. Carb. Polym. 79, 414–417. https://doi.org/10.1016/j.carbpol.2009.08.027.

Ju, X.-M., Wang, D.-H., Zhang, G.-C., Cao, D., Wei, G.-Y., 2015. Efficient pullulan production by bioconversion using *Aureobasidium pullulans* as the whole-cell catalyst. Appl. Microbiol Biotechnol. 99, 211–220. https://doi.org/10.1007/s00253-014-6100-1.

Kang, L., Liang, Q., Rashid, A., Qayum, A., Chi, Z., Ren, X., Ma, H., 2023. Ultrasound-assisted development and characterization of novel polyphenol-loaded pullulan/trehalose composite films for fruit preservation. Ultrason. Sonochem. 92, 106242. https://doi.org/10.1016/j.ultsonch.2022.106242.

Karaca, H., Pérez-Gago, M.B., Taberner, V., Palou, L., 2014. Evaluating food additives as antifungal agents against Monilinia fructicola in vitro and in hydroxypropyl methylcellulose–lipid composite edible coatings for plums. Int. J. Food Microbiol 179, 72–79. https://doi.org/10.1016/j.ijfoodmicro.2014.03.027.

Karim, M.R., Islam, Md.S., 2011. Thermal behavior with mechanical property of fluorinated silane functionalized superhydrophobic pullulan/poly(vinyl alcohol) blends by electrospinning method. J. Nanomat. 2011, 1–7. https://doi.org/10.1155/2011/979458.

Kumar, P., Sethi, S., Sharma, R.R., Srivastav, M., Singh, D., Varghese, E., 2018. Edible coatings influence the cold-storage life and quality of 'Santa Rosa' plum (*Prunus salicina* Lindell). J. Food Sci. Technol. 55, 2344–2350. https://doi.org/10.1007/s13197-018-3130-1.

Kumar, N., Pratibha, Prasad, J., Yadav, A., Upadhyay, A., Neeraj, S., Kieliszek, M., 2023. Recent trends in edible packaging for food applications—perspective for the future. Food Eng. Rev. 15 (4), 718–747.

Lieu, M.D., Phuong, T.V., Nguyen, T.T.B., Dang, T.K.T., Nguyen, T.H., 2024. A review of preservation approaches for extending avocado fruit shelf-life. J. Agr. Food Res. 16, 101102. https://doi.org/10.1016/j.jafr.2024.101102.

Luís, Â., Ramos, A., Domingues, F., 2020. Pullulan films containing rockrose essential oil for potential food packaging applications. Antibiotics 9, 681. https://doi.org/10.3390/antibiotics9100681.

Marín, A., Cháfer, M., Atarés, L., Chiralt, A., Torres, R., Usall, J., Teixidó, N., 2016. Effect of different coating-forming agents on the efficacy of the biocontrol agent *Candida sake* CPA-1 for control of Botrytis cinerea on grapes. Biol. Control 96, 108–119. https://doi.org/10.1016/j.biocontrol.2016.02.012.

Marsh, K., Bugusu, B., 2007. Food packaging - Roles, materials, and environmental issues: Scientific status summary. J. Food Sci. 72 (3). https://doi.org/10.1111/j.1750-3841.2007.00301.x.

Miranda, M., Bai, J., Pilon, L., Torres, R., Casals, C., Solsona, C., Teixidó, N., 2024. Fundamentals of edible coatings and combination with biocontrol agents: a strategy to improve postharvest fruit preservation. Foods 13, 2980. https://doi.org/10.3390/foods13182980.

Mishra, B., Suneetha, V., Rath, K., 2011. The role of microbial pullulan, a biopolymer in pharmaceutical approaches: a review. J. Appl. Pharm. Sci. 1 (2011), 45–50.

Muszkieta, L., Carrion, S.D.J., Robinet, P., Beau, R., Elbim, C., Pearlman, E., Latgé, J.-P., 2014. The protein phosphatase PhzA of *A. fumigatus* is involved in oxidative stress tolerance and fungal virulence. Fungal Gen. Biol. 66, 79–85. https://doi.org/10.1016/j.fgb.2014.02.009.

Pooja Saklani, P.S., Nath, S., Kishor Das, S., Singh, S.M., 2019. A review of edible packaging for foods. Int. J. Curr. Microbiol. Appl. Sci. 8, 2885–2895. https://doi.org/10.20546/ijcmas.2019.807.359.

Poudel, D., Swilley-Sanchez, S., O'keefe, S., Matson, J., Long, T., Fernández-Fraguas, C., 2020. Novel electrospun pullulan fibers incorporating hydroxypropyl-β-cyclodextrin: morphology and relation with rheological properties. Polymers 12, 2558. https://doi.org/10.3390/polym12112558.

Prajapati, V.D., Jani, G.K., Khanda, S.M., 2013. Pullulan: an exopolysaccharide and its various applications. Carb. Polym. 95, 540–549. https://doi.org/10.1016/j.carbpol.2013.02.082.

Prasongsuk, S., Berhow, M.A., Dunlap, C.A., Weisleder, D., Leathers, T.D., Eveleigh, D.E., Punnapayak, H., 2007. Pullulan production by tropical isolates of *Aureobasidium pullulans*. J. Ind. Microbiol. Biotechnol. 34, 55–61.

Raychaudhuri, R., Naik, S., Shreya, A.B., Kandpal, N., Pandey, A., Kalthur, G., Mutalik, S., 2020. Pullulan based stimuli responsive and sub cellular targeted nanoplatforms for biomedical application: synthesis, nanoformulations and toxicological perspective. Int. J. Biol. Macromol. 161, 1189–1205.

Saber-Samandari, Samaneh, Gulcan, H.O., Saber-Samandari, Saeed, Gazi, M., 2014. Efficient removal of anionic and cationic dyes from an aqueous solution using pullulan-graft-polyacrylamide porous hydrogel. Water Air Soil Pollut. 225, 2177. https://doi.org/10.1007/s11270-014-2177-5.

Sánchez-González, L., Quintero Saavedra, J.I., Chiralt, A., 2013. Physical properties and antilisterial activity of bioactive edible films containing *Lactobacillus plantarum*. Food Hydrocoll. 33, 92–98.

Sánchez-González, L., Quintero Saavedra, J.I., Chiralt, A., 2014. Antilisterial and physical properties of biopolymer films containing lactic acid bacteria. Food Control 35, 200–206.

Settier-Ramírez, L., López-Carballo, G., Hernández-Muñoz, P., Fontana-Tachon, A., Strub, C., Schorr-Galindo, S., 2022. Apple-based coatings incorporated with wild apple isolated yeast to reduce Penicillium expansum postharvest decay of apples. Postharvest Biol. Technol. 185, 111805. https://doi.org/10.1016/j.postharvbio.2021.111805.

Shah, A., Ashames, A.A., Buabeid, M.A., Murtaza, G., 2020. Synthesis, in vitro characterization and antibacterial efficacy of moxifloxacin-loaded chitosan-pullulan-silver-nanocomposite films. J. Drug Del. Sci. Technol. 55, 101366. https://doi.org/10.1016/j.jddst.2019.101366.

Shingel, K.I., 2002. Determination of structural peculiarities of dexran, pullulan and g-irradiated pullulan by Fourier-transform IR spectroscopy. Carb. Res.

Singh, R.S., Kaur, N., 2019. Understanding response surface optimization of medium composition for pullulan production from de-oiled rice bran by *Aureobasidium pullulans*. Food Sci. Biotechnol. 28, 1507–1520. https://doi.org/10.1007/s10068-019-00585-w.

Singh, R.S., Kaur, N., Kennedy, J.F., 2019. Pullulan production from agro-industrial waste and its applications in food industry: a review. Carb. Polym. 217, 46–57.

Sugumaran, K.R., Ponnusami, 2017. Review on production, downstream processing and characterization of microbial pullulan. Carb. Polym. 173, 573–591. https://doi.org/10.1016/j.carbpol.2019.04.050.

Synytsya, A., Novak, M., 2014. Structural analysis of glucans. Ann. Transl. Med. 2, 2 (February 27, 2014): Ann. Transl. Med. (Beta-glucan).

Tulukoğlu-Kunt, K.S., Özden, M., Di Francesco, A., 2023. Exploring wild and local fruits as sources of promising biocontrol agents against alternaria spp. in apples. Horticulturae 9, 1156. https://doi.org/10.3390/horticulturae9101156.

Wang, D., Chen, F., Wei, G., Jiang, M., Dong, M., 2015. The mechanism of improved pullulan production by nitrogen limitation in batch culture of *Aureobasidium pullulans*. Carb. Polym. 127, 325–331. https://doi.org/10.1016/j.carbpol.2015.03.079.

Wani, S.M., Mir, S.A., Khanday, F.A., Masoodi, F.A., 2021. Advances in pullulan production from agro-based wastes by *Aureobasidium pullulans* and its applications. Inn. Food Sci. Emerg. Technol. 74, 102846. https://doi.org/10.1016/j.ifset.2021.102846.

Yadav, A., Kumar, N., Upadhyay, A., Fawole, O.A., Mahawar, M.K., Jalgaonkar, K., Chandran, D., Rajalingam, S., Zengin, G., Kumar, M., Mekhemar, M., 2022. Recent advances in novel packaging technologies for shelf-life extension of guava fruits for retaining health benefits for longer duration. Plants 11, 547. https://doi.org/10.3390/plants11040547.

Yuen, S., 1974. Pullulan and its applications. Process Biochem. 9, 22.